Formosa, N. and Scerri, K. (2015). *Xjenza Online*, 3:23–30.

Xjenza Online - Journal of The Malta Chamber of Scientists
www.xjenza.org
DOI: 10.7423/XJENZA.2015.1.03

Research Article

Real-Time Modelling and Interpolation of Spatio-Temporal Marine Pollution

N. Formosa, K. Scerri
University of Malta, Faculty of Engineering

Abstract. Due to the complexity of the interactions involved in various dynamic systems, known physical, biological or chemical laws cannot adequately describe the dynamics behind these processes. The study of these systems thus depends on measurements often taken at various discrete spatial locations through time by noisy sensors. For this reason, scientists often necessitate interpolative, visualisation and analytical tools to deal with the large volumes of data common to these systems. The starting point of this study is the seminal research by C. Shannon on sampling and reconstruction theory and its various extensions. Based on recent work on the reconstruction of stochastic processes, this paper develops a novel real-time estimation method for non-stationary stochastic spatio-temporal behaviour based on the Integro-Difference Equation (IDE). This methodology is applied to collected marine pollution data from a Norwegian fjord. Comparison of the results obtained by the proposed method with interpolators from state-of-the-art Geographical Information System (GIS) packages will show, that significantly superior results are obtained by including the temporal evolution in the spatial interpolations.

1 Introduction

Complex spatio-temporal interactions are exhibited in various natural systems as witnessed in ecology, meteorology, physics and epidemiology. Such natural systems evolve on a continuous spatial domain, but the data sets collected from these systems are made up of spatially localised measurements taken at different discrete spatial locations through time by noisy sensors. Nevertheless, for analysis and visualisation purposes, the underlying, spatially continuous processes must often be reconstructed from these discrete measurements.

Traditionally, spatial interactions have been mathematically explained using spatial models, and several interpolation techniques are readily available. Nevertheless, these methods provide interpolations that ignore the temporal behaviour of the process. Typical examples include Inverse Distance Weighting (IDW) (Poshtmasari, Sarvestani, Kamkar, Shataei & Sadeghi, 2012), Gaussian Radial Basis Functions (GRBF) (Poshtmasari et al., 2012) and Kriging (Poshtmasari et al., 2012; Schabenberger & Gotway, 2005). However, since spatial measurements are also often repeatedly taken in time, any interpolated field could greatly benefit from augmenting the temporal evolution of the data with the spatial information. A modern approach to the interpolation from spatial-temporal information may be based on the reconstruction step of sampling theory first attributed to C. Shannon's seminal work (Shannon, 1949). The aim of this paper is thus to provide a novel real-time procedure for the estimation of the underlying stochastic process from noisy observations that serves as a new tool for better interpolations. Another significant contribution is the validation of the developed methods on a pollution data set highlighting the applicability of this methodology to real-world applications.

The remainder of this paper is structured as follows. The historical developments of sampling and reconstruction theory fundamental to this research are presented in Section II. More recent developments required for this work together with the chosen real-time estimation approach are presented in Section III. Section IV is dedicated to an illustrative example highlighting the benefits of this procedure. Finally, some concluding remarks are drawn together with an overview of some possible future additions in Section V.

Correspondence to: N. Formosa (nicolette.formosa@um.edu.mt)

2 Historical Developments

The starting point of this research is the seminal study by C. Shannon on sampling and reconstruction theory and its various extensions. Shannon first presented the fundamental framework to represent a bandlimited, continuous time signal as a discrete sequence without any loss of information in 1949 (Shannon, 1949). He also introduced an approach for a perfect reconstruction of the original time signal from its sampled representation. Over the past decades, Shannon's work has been extended by various notable contributors as summarised by M. Unser in (Unser, 2000). These extensions aim to relax some of Shannon's assumptions and extend the framework to account for non-ideal sampling (S. Ramani D. Van De Ville & Unser, 2008), multidimensional settings (Petersen & Middleton, 1962; Izen, 2005; Feuer, 2004; Jr. & Sangsari, 1989) and more convenient reconstruction spaces (Yao, 1967; Eldar & Unser, 2006; Eldar & Werther, 2005; Nashed & Walter, 1991). Table 1 summarises the main contributions to sampling and reconstruction theory published since the seminal work of Shannon together with the contributions envisaged through this work.

The restriction to unidimensional processes assumed in Shannon's sampling theory prevents the application of this seminal theory to multidimensional signals. Petersen et. al. (Petersen & Middleton, 1964) extended this theory to accommodate other areas where physical phenomena need to be measured in a multidimensional continuum. Some conspicuous fields within this area include meteorology, oceanography, seismology, acoustics, optics and radar (Petersen & Middleton, 1962). Papoulis (Papoulis, 1977) continued Shannon's work stating that it is unrealistic to assume that the acquisition device is ideal. The theory thus developed shows the introduction of a non-ideal acquisition device prior to sampling. However due to the introduction of a non-ideal acquisition device, a discrete correction filter prior to the reconstruction stage is required to limit its effect.

Moreover, sampling, as presented by Shannon is restricted to bandlimited signals. However, for non-bandlimited signals, Aldroubi and Unser (Aldroubi, Unser & Aldroubi, 1994) proposed the use of alternative reconstruction spaces which take into account both the input signal and the sampling process. Conventional sampling and interpolation theories provide solutions to the problem of reconstructing a signal from its samples limited to a noise-free scenario. Perfect reconstruction can, therefore, be achieved as long as this noise free acquisition is respected. In any real world application, the measured signals are always corrupted by various degrees of noise levels and, therefore, perfect reconstruction is no longer attainable. Eldar and Unser in (Eldar & Unser, 2006), therefore, proposed the use of the Weiner filter as the discrete correction filter to limit the effect of measurement noise on the reconstruction process.

Classical sampling theory assumes that each realisation of the sampling processes is independent of all past signals. Wikle showed that although such an assumption is valid in various temporal or spatial applications, it is violated for spatio-temporal signals where successive spatial samples are temporally related to the dynamics of the process under observation (Wikle, 2002). Thus, sampling and reconstruction theory of non-stationary stochastic processes utilises a dynamic filter to capture the temporal evolution of the process (Scerri, Dewar & Kadirkamanathan, 2008).

Building on the extensions discussed in this section, this work provides a method for the reconstruction of sampled non-stationary stochastic processes observed in the presence of noise. A modern shift-invariant approach is also adopted in a multi-dimensional domain. The sampling and reconstruction methods developed in this paper are based on the same building blocks as presented in (Scerri et al., 2008). Nevertheless, this research extends the work in (Scerri et al., 2008) such that the estimation of the kernel from noisy observations is implemented in real-time. As opposed to previous work, the methods developed were validated on collected marine pollution measurements.

3 Theoretical Developments

The temporally evolving signal $z(\mathbf{s},t) \in L_2 \ \forall \ t$ where L_2 is the space of measurable, square-integrable, real-valued functions with $\mathbf{s} \in \mathbb{R}^n$ and $t \in \mathbb{Z}^+$. The signal $z(\mathbf{s},t)$ is continuous in the spatial domain $(\mathbf{s})$ but discrete in the temporal domain (t).

As done in (Scerri et al., 2008), an approximation to the spatially continuous signal $z(\mathbf{s},t)$ in the shift invariant space V, is given by this projection into V given by

$$z(\mathbf{s},t) \approx \sum_{j\in\mathbb{Z}} \langle z(\mathbf{s},t), \phi_{x_j}(\mathbf{s})\rangle \phi_{x_j}(\mathbf{s}) = \mathbf{x}(t)^\top \boldsymbol{\phi}_x(\mathbf{s}) \quad (1)$$

where

$$\begin{aligned} \mathbf{x}(k,t) &= [\langle z(\mathbf{s},t), \phi_{x_1}(\mathbf{s})\rangle \ \ \ldots \ \ \langle x(\mathbf{s},t), \phi_{x_{n_x}}(\mathbf{s})\rangle]^\top \\ \boldsymbol{\phi}_i(\mathbf{s}) &= [\phi_{i_1}(\mathbf{s}) \ \ \ldots \ \ \phi_{i_{n_i}}(\mathbf{s})]^\top \end{aligned} \quad (2)$$

$\phi_i(\mathbf{s})$ is some chosen reconstruction function. In this work it is assumed that the temporal evolution of the stochastic process $z(\mathbf{s},t)$ can be described by the linear spatial convolution of the previous field with an unknown kernel $k(\mathbf{s})$ and subject to some additive noise process given by:

$$z(\mathbf{s},t) = \int z(.,t-1)k(.) + \eta(\mathbf{s},t) \quad (3)$$

Table 1: Comparison of the various extensions to Shannon's sampling theorem.

Method	Dimensions	Acquisition Device	Reconstruction Space	Dynamics	Noise	Real-Time
(Shannon, 1949)	1-D	Ideal	Bandlimited	No	No	No
(Petersen & Middleton, 1964)	Multi-D	Ideal	Bandlimited	No	No	No
(Papoulis, 1977)	1-D	Non-ideal	Bandlimited	No	No	No
(Aldroubi, Unser & Aldroubi, 1994)	1-D	Non-ideal	Shift-Invariant	No	No	No
(Wikle, 2002)	1-D	Non-ideal	Harmonic	Yes	No	No
(Eldar & Unser, 2006)	1-D	Non-ideal	Shift-invariant	No	Yes	No
(Scerri, Dewar & Kadirkamanathan, 2008)	Multi-D	Non-ideal	Shift-invariant	Yes	Yes	No
This research (2014)	Multi-D	Non-ideal	Shift-invariant	Yes	Yes	Yes

where $\eta(\mathbf{s},t)$ is a zero mean stationary Gaussian noise process with covariance Σ_η given by

$$\Sigma_\eta = \mathrm{COV}[z(\mathbf{s},t), z(\mathbf{s}+\mathfrak{s}, t+\mathfrak{t})] = \begin{cases} \lambda(\mathfrak{s}) & \text{if } \mathfrak{t}=0 \\ 0 & \text{otherwise} \end{cases} \tag{4}$$

Sampling is performed where filtering by the non-ideal acquisition device is followed by an ideal sampler. The output of the non-ideal filter is dictated by its impulse response, $h(\mathbf{s})$, and is given by:

$$y(\mathbf{s}_i,t) = \int_{\mathcal{S}} h(\mathbf{s}_i - \mathbf{r}) z(\mathbf{r},t) d\,\mathbf{r} + v(t) \tag{5}$$

where $v(t)$ is a zero mean white Gaussian noise process uncorrelated with $\eta(\mathbf{s},t)$ representing measurement noise.

A major difficulty in making use of the unknown temporal dynamics in the reconstruction of $z(\mathbf{s},t)$ is the continuous nature of the convolution describing the temporal dynamics as given by (3). An approximate discretised representation of the dynamics (3) and the observation process (5) can be obtained by considering the approximations:

$$z(\mathbf{s},t) \approx \sum_{j=1}^{n_x} \langle z(\mathbf{s},t), \phi_{x_j}(\mathbf{s})\rangle \phi_{x_j}(\mathbf{s}) = \mathbf{x}(t)^\top \boldsymbol{\phi}_x(\mathbf{s}) \tag{6}$$

$$k(\mathbf{s}) \approx \sum_{j=1}^{n_\theta} \langle k(\mathbf{s}), \phi_{\theta_j}(\mathbf{s})\rangle \phi_{\theta_j}(\mathbf{s}) = \boldsymbol{\theta}^\top \boldsymbol{\phi}_\theta(\mathbf{s}) \tag{7}$$

$$h(\mathbf{s}) \approx \sum_{j=1}^{n_\vartheta} \langle h(\mathbf{s}), \phi_{\vartheta_j}(\mathbf{s})\rangle \phi_{\vartheta_j}(\mathbf{s}) = \boldsymbol{\vartheta}^\top \boldsymbol{\phi}_\vartheta(\mathbf{s}) \tag{8}$$

$$\lambda(\mathbf{s}) \approx \sum_{j=1}^{n_\varrho} \langle \lambda(\mathbf{s}), \phi_{\varrho_j}(\mathbf{s})\rangle \phi_{\varrho_j}(\mathbf{s}) = \boldsymbol{\varrho}^\top \boldsymbol{\phi}_\varrho(\mathbf{s}) \tag{9}$$

where

$$\begin{aligned} \mathbf{x}(t) &= [\langle z(\mathbf{s},t), \phi_{x_1}(\mathbf{s})\rangle \quad \dots \quad \langle x(\mathbf{s},t), \phi_{x_{n_x}}(\mathbf{s})\rangle]^\top \\ \boldsymbol{\theta} &= [\langle k(\mathbf{s}), \phi_{\theta_1}(\mathbf{s})\rangle \quad \dots \quad \langle k(\mathbf{s}), \phi_{\theta_{n_\theta}}(\mathbf{s})\rangle]^\top \\ \boldsymbol{\vartheta} &= [\langle h(\mathbf{s}), \phi_{\vartheta_1}(\mathbf{s})\rangle \quad \dots \quad \langle h(\mathbf{s}), \phi_{\vartheta_{n_\vartheta}}(\mathbf{s})\rangle]^\top \\ \boldsymbol{\varrho} &= [\langle \lambda, (\mathbf{s})\phi_{\varrho_1}(\mathbf{s})\rangle \quad \dots \quad \langle \lambda(\mathbf{s}), \phi_{\varrho_{n_\varrho}}(\mathbf{s})\rangle]^\top \\ \boldsymbol{\phi}_i(\mathbf{s}) &= [\phi_{i_1}(\mathbf{s}) \ \dots \ \phi_{i_{n_i}}(\mathbf{s})]^\top \end{aligned} \tag{10}$$

Based on these decompositions an approximate discrete representation of the dynamics (3) and the non-ideal sampler (5) with known error bounds is given by Theorem 1 (Scerri et al., 2008).

Theorem 1. *Using the spatially discrete representations (6) to (9), the dynamic equation (3) and the observation equation (5) can be approximated by the finite dimension state-space model*

$$\mathbf{x}(t+1) = A(\boldsymbol{\theta})\,\mathbf{x}(t) + \mathbf{w}(t) \tag{11}$$

and

$$\mathbf{y}(t) = C(\boldsymbol{\vartheta})\,\mathbf{x}(t) + \mathbf{v}(t) \tag{12}$$

where

$$A(\boldsymbol{\theta}) = \Psi^{-1} \int_{\mathcal{S}} \boldsymbol{\phi}_x(\mathbf{s})\,\boldsymbol{\theta}^\top\,\Xi_\theta(\mathbf{s}) d\mathbf{s} \tag{13}$$

$$\Psi = \int_{\mathcal{S}} \boldsymbol{\phi}_x(\mathbf{s})\,\boldsymbol{\phi}_x(\mathbf{s})^\top d\mathbf{s} \tag{14}$$

$$\Xi_\theta(\mathbf{s}) = \int_{\mathcal{S}} \boldsymbol{\phi}_\theta(\mathbf{s}-\mathbf{r})\,\boldsymbol{\phi}_x(\mathbf{r})^\top d\,\mathbf{r} \tag{15}$$

$$C(\boldsymbol{\vartheta}) = \begin{pmatrix} \boldsymbol{\vartheta}^\top\,\Xi_\vartheta(\mathbf{s}_1) \\ \vdots \\ \boldsymbol{\vartheta}^\top\,\Xi_\vartheta(\mathbf{s}_{n_y}) \end{pmatrix}$$

$$\Xi_{\vartheta}(\mathbf{s}) = \int_{\mathcal{S}} \boldsymbol{\phi}_{\vartheta}(\mathbf{s}-\mathbf{r})\, \boldsymbol{\phi}_{x}(\mathbf{r})^{\top} d\,\mathbf{r} \tag{16}$$

$$\mathbf{w}(t) \sim \mathcal{N}(0, \Sigma_w) \tag{17}$$

with

$$\Sigma_w = \Psi^{-1} \int_{\mathcal{S}} \boldsymbol{\phi}_{\varrho}(\mathbf{s}) \varrho(\mathbf{s})^{\top} \Xi_{\varrho}(\mathbf{s}) d\mathbf{s} \Psi^{-\top} \tag{18}$$

$$\Xi_{\varrho}(\mathbf{s}) = \int_{\mathcal{S}} \boldsymbol{\phi}_{\varrho}(\mathbf{s}-\mathbf{r})\, \boldsymbol{\phi}_{x}(\mathbf{r})^{\top} d\,\mathbf{r} \tag{19}$$

and $\mathbf{v}(t) \sim \mathcal{N}(0, \Sigma_v)$ *with* $\Sigma_v = \sigma_v I_{n_y}$*; with errors in the approximation of* $z(\mathbf{s}, t)$ *given by*

$$\epsilon_z = |z(\mathbf{s},t) - \mathbf{x}(t)^{\top}\, \boldsymbol{\phi}_x(\mathbf{s})| \leqslant \epsilon'_z \int_{\mathbb{R}^n : \boldsymbol{\nu} > \boldsymbol{\nu}_c} \Phi_x(\boldsymbol{\nu}) d\,\boldsymbol{\nu} \tag{20}$$

where

$$\epsilon'_z = \sup_{\mathbb{R}^n : \boldsymbol{\nu} > \boldsymbol{\nu}_c} |Z(\boldsymbol{\nu}) \Phi_x^{-1}(\boldsymbol{\nu})| \tag{21}$$

Proof is found in (Scerri et al., 2008). Since the dynamics are unknown, a joint estimation technique is being proposed to simultaneously reconstruct both the stochastic non-stationary spatio-temporal process and the systems dynamics from the noise-corrupted observations. This research necessitates real-time learning of the model parameters and states, with the most widely used techniques being the online version of the Expectation-Maximisation (EM) algorithm, particle filters and the Dual Kalman filter. Despite being a mathematically rigorous technique, the online version of the EM algorithm is not easily applicable to different solutions due to the possible intractability of the maximisation function (Ozkan, Fritsche & Gustafsson, 2012). On the other hand, although particle filters are easily applicable to varied dynamics and provide accurate and rigorous solutions, they carry a significant computational burden which can easily become excessive in a spatio-temporal setting (Kwok, Fox & Meila, 2004). Thus, the dual Kalman filter was chosen for this application due to its low computational cost, easy of adoption, rapid convergence and well-studied behaviour (Wan, van der Merwe & Nelson, 1999).

The state estimates based upon the initial estimates of $\boldsymbol{\theta}$ are obtained from the first state space representation given in (3) and (12). Estimates of the parameter $\boldsymbol{\theta}$ based on the values from first state-space model, are then obtained from the state space representation given by:

$$\boldsymbol{\theta}(t+1) = I\boldsymbol{\theta}(t) + \mathbf{q}(t) \tag{22}$$

$$x(t+1) = B(x(t))\boldsymbol{\theta} + \mathbf{w}(t) \tag{23}$$

Note that (23) is a rewriting of (11) as done in (Scerri et al., 2008). This completes one run of the algorithm. Therefore, the use of dual Kalman filtering based on the state space model describing both the states and parameter evolution in real-time leads to the reconstruction of the spatio-temporal process $z(\mathbf{s}, t)$. Note that, the sensor's spatial characteristics are assumed to be known when the spatio-temporal process and the model dynamics are being inferred. Such an assumption is reasonable since sensor characteristics may be either given by the manufacturer or measured by experimentation. Nevertheless, this assumption may be relaxed by adding the estimation of the sensors parameters, $\boldsymbol{\vartheta}$, to the dual estimation procedure.

4 Marine Pollution Spread Modelling and Interpolation

An important contribution of this research was to apply the developed models on a real data set. To the author's best knowledge, this is the first application of such a methodology to real data. The marine pollution dataset was provided by NORUS, a north American and Norwegian educational programme (Medina, Moline, Clark & Wood, 2011). Its main focus is the study of the effect of climate change on the ecosystems and living organisms. Part of the data required for NORUS is obtained via the Slocum Glider (Medina et al., 2011), an autonomous underwater robot.

The dataset used for this project was taken from this glider deployed in the fjord of Svalbard, Norway. The glider's mission extended from longitude 13.3042° East to 16.6875° East and latitude 78.1042° North and 78.7042° North (Medina et al., 2011). During the 17-day mission, which began on June 30, 2009, the glider collected a large data set of measurements for each of its 20 onboard sensors. The data set available for this research includes the position of the glider and the oxygen concentration at the robot's location and the time of measurement. Oxygen concentration is an important indicator of water quality, and it is envisaged that this methodology can adequately capture its spatio-temporal evolution from the measured data in real time. Such behaviour is similar to other spreading pollutants in large bodies of water which may necessitate real-time spatio-temporal interpolation and prediction in the natural disaster scenarios.

4.1 Pre-Processing of Data

The stochastic spatio-temporal measurement of interest in this research is the oxygen concentration. Thus, these measurements were plotted against their discrete sampling instances as shown in Figure 1. This plot shows variations in oxygen concentrations with time as the glider is moving and collecting the data. It indic-

ates that there exists a cyclical variation in the oxygen readings.

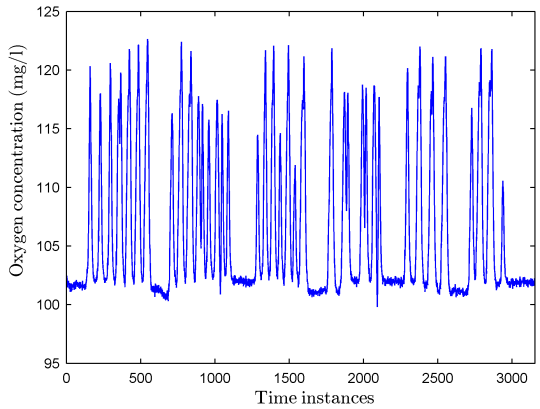

Figure 1: Oxygen concentration plotted against time.

With the aim to visualise the main causes of the cyclic variations in oxygen concentration, a similar graph of the depth against the time instances is shown in Figure 2 . Both Figures 1 and 2 are seen to exhibit very similar behaviour, each having similar cycles at the same time instances. This highlights the strong relationship between oxygen concentration and depth.

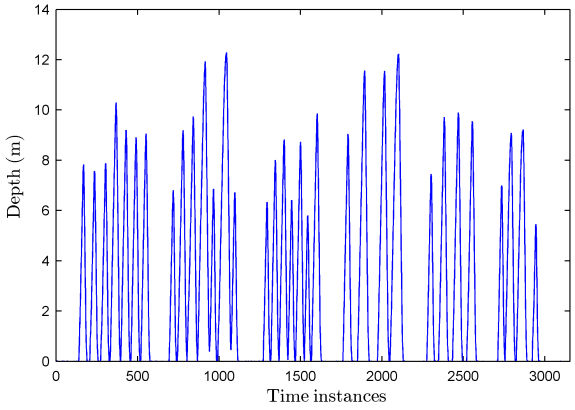

Figure 2: Depth variation as the glider is moving in time.

A detrending procedure was carried out to capture the apparent relationship between the oxygen level and the depth. Detrending is often applied to remove a feature thought to distort or obscure the relationships of interest (Chatfield, 2004). After detrending, to facilitate interpretation and modelling of the dataset, trend estimation was carried out. In trend estimation, a model is developed to pick up the main characteristics of the data. Based on this pre-processing procedure, the residuals were clustered into four groups, with models for each cluster given by:

- Cluster 1

$$l(t) = m_1 + c_1 d + r(t) \tag{24}$$

- Cluster 2

$$l(t) = m_2 + c_2 d + r(t) \tag{25}$$

- Cluster 3

$$l(t) = m_3 + r(t) \tag{26}$$

- Cluster 4

$$l(t) = m_4 + r(t) \tag{27}$$

where $l(t)$ is the oxygen level, d is the depth, m is the mean of the data, c is the linear regression model parameter and $r(t)$ represents the residual left after detrending. Using Least Squares estimation, the model parameters obtained are presented in Table 2.

Table 2: Simulation function and parameters.

Parameter	Value
m_1	3.1947
c_1	1.2115
m_2	−1.1732
c_2	−0.9596
m_3	1.0678
m_4	−8.6269

A plot of the detrended version of the original data set is given in Figure 3. This figure indicates that the residuals form a horizontal band about zero and have a very small variance up to a depth of 6m. Moving, however, to a greater depth, even though the mean remains around zero, the variance is significantly larger.

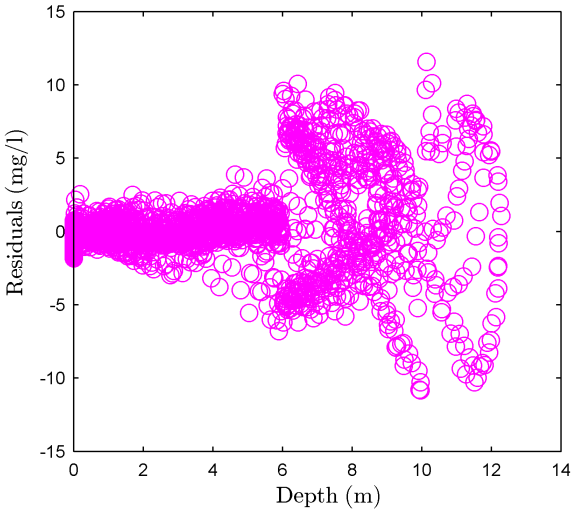

Figure 3: Detrended Data.

To verify if significant spatial and temporal correlations are still present after detrending, correlation coefficients are obtained. The correlogram presented in Figure 4, facilitates the interpretation of the results of the autocorrelation coefficients. The 95% confidence intervals are also included in Figure 4. Values outside these confidence intervals are considered to be statistically insignificant. Figure 4 shows that significant spatial and temporal correlations still exist in the residues since values at low lag exhibit correlation coefficients well beyond the 95% confidence interval.

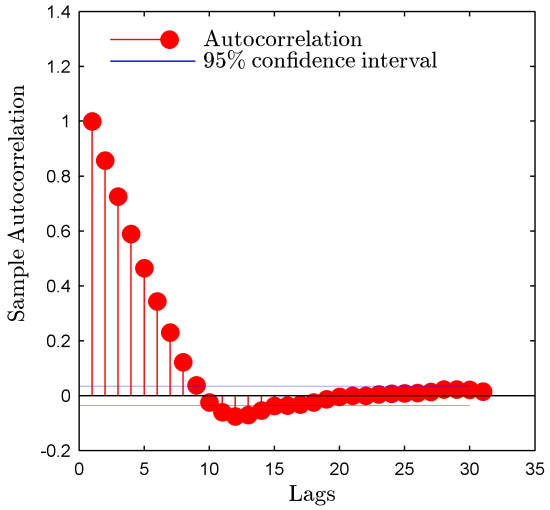

Figure 4: Correlogram for the Detrended Data.

4.2 Spatio-Temporal Modelling

Since the pollution spread dynamics are unknown, the reconstruction being proposed reconstructs both the spatio-temporal process and the model kernel via the joint estimation technique in real-time. This is carried out based on the spatial location of the measurements and their evolution through time. Fourier and correlation analysis were used to identify the bandwidth and kernel support of the data as suggested in (Scerri et al., 2008). Based on this analysis, a spatio-temporal model was proposed using cubic B-splines as the basis functions. The functions and parameters for reconstruction of both the process and the underlying dynamics are presented in Table 3.

The tests carried out on the proposed interpolation technique measure the accuracy of the spatio-temporal interpolation. To quantify the accuracy of the reconstructed spatio-temporal process, Table 4 shows the Root Mean Square Error (RMSE) difference between the measured spatio-temporal process and the reconstructed process. These RMSE measures indicate relatively small errors between the measurements and the reconstructed field. The values from Table 4 show that for the randomly chosen time points, the proposed methodology for real-time estimation of the parameters and the states obtained a reasonably smoothed representation of the measured data. Running on standard computer hardware with Intel(R) Core(TM) i7-2670QM CPU at 2.20GHz processor and 8GB of main memory, the computational time for each time point was approximately 0.388s, thus near immediate estimates are obtained for each now measured field. Most importantly, the overall RMSE over all time points is measured at 0.5345mg/l, indicating that the proposed procedure for real-time parameter and state estimation was able to pick the main process behaviour at each time and the interpolated behaviour is a good representative sample of the general behaviour.

Table 3: Simulation function and parameters.

Function and Parameter		Simulation Value
$\lambda(\mathbf{s})$	=	$\delta(\mathbf{s})$
$h(\mathbf{s})$	=	$0.3\ \exp(\frac{\mathbf{s}^2}{3})$
n_y	=	3134
n_θ	=	3
n_ϑ	=	3
$n_x = n_\rho$	=	7
basis locations for $z(\mathbf{s},t)$	=	$\{-11,-7.5,...,10\}$
basis locations for $k(\mathbf{s})$	=	$\{-3.5,0,3.5\}$
basis locations for $h(\mathbf{s})$	=	$\{-3.5,0,3.5\}$

The widely used 10-fold validation method (McLachlan, Do & Ambroise, 2004) is used as a validation of the proposed methodology. Thus, a sample of 300-time points is removed from the data set for each run to be used as a validation set. The advantage of this method is that all observations are used for both training and validation, and each observation is used for validation only once. The RMSE of each fold used as a validation set is presented in Table 5. For each fold, the results show that good estimates are obtained with low RMSEs and relatively low percentage errors. Moreover for each fold tested, the kernel parameters converged to the same values, obtaining a repeatable kernel reconstruction.

4.3 Comparison with Other Interpolation Techniques

Furthermore, standard spatial interpolation techniques provided by the latest GIS software were used to compare their performance with the results obtained from the proposed real-time methodology. 10-fold validation was carried out for each interpolation technique available in GIS software. The results from each interpolation technique are included in Table 6 together with the spatio-temporal methodology developed in this pa-

Table 4: RMSE of the reconstructed spatio-temporal process for the randomly chosen time points.

t	RMSE (mg/l)	% error	t	RMSE (mg/l)	% error
89	0.5004	0.4924	162	2.0910	1.9366
332	0.5366	0.4910	520	1.2928	1.1600
787	0.2517	0.2444	890	2.1250	2.7420
1222	0.2904	0.2851	1329	1.2021	1.7563
1546	0.3534	0.3440	1800	0.5198	0.5072
1844	0.3303	0.3125	1963	0.2165	0.2090
2385	1.0642	1.0048	2855	2.6440	2.1341
3005	0.3193	0.3135	3118	0.3247	0.3188

Table 5: Overall RMSE of the reconstructed spatio-temporal process within each fold.

t	RMSE (mg/l)	% error
1:300	0.2054	0.2015
301:600	0.2942	0.2797
601:900	0.3711	0.3506
901:1200	0.4049	0.3826
1201:1500	0.2956	0.2786
1501:1800	0.2396	0.2260
1801:2100	0.3085	0.2906
2101:2400	0.1649	0.1555
2401:2700	0.2205	0.2082
2701:3000	0.2262	0.2133

per. These results show that the lowest RMSE from all standard interpolation techniques is obtained via empirical Bayesian kriging. Nevertheless, this is still significantly outperformed by the spatio-temporal methodology developed in this paper.

Table 6: Summary of the results for all the interpolators which were considered.

All Functions in GIS software and developed models	RMSE (mg/l)
Inverse Distance Weighting	1.0521
Global Polynomial Interpolation - Order 10	2.1503
Radial Basis Functions - Multiquadratic Kernel	1.0156
Local Polynomial Interpolator - Order 1 with Exponential Kernel	1.7826
Kriging/CoKriging - Ordinary Kriging	1.0283
Kriging/CoKriging - Universal Kriging	1.0283
Empirical Bayesian Kriging	0.9862
Diffusion Kernel	2.0332
Spatio-Temporal Modelling	0.2731

5 Conclusion

This research presented a structured approach to data-driven spatio-temporal modelling and spatial interpolation utilising a state space representation of the IDE with parameter and state estimation in real-time. Classical interpolation theory assumes that the data collected from sensors is independent of all past signals. However, in spatio-temporal signals, successive spatial samples are temporally related based on the dynamics of the process under observation. Novel methods for modelling and spatial interpolation were developed based on multidimensional sampling theory, to cater for noise-corrupted observations from spatially discrete sensors. A real-time estimation procedure was utilised to estimate the model dynamics and the hidden spatio-temporal process with the use of the dual Kalman filter. This methodology was applied to a real data set thus providing the very first validation of these methods on gathered, rather than simulated data. The proposed models together with the methodology developed, obtained better interpolative results than any competitive spatial interpolator. This can be attributed to the use of the temporal information in the developed interpolator. Thus, these spatio-temporal models may aid in both the visualisations of the data and a better understanding of the evolving process.

To further enhance the applicability of the proposed methodology, various other extensions could be considered. In one such extension, the assumptions of full knowledge of the spatial response of the sensor and the support of the continuous functions of the IDE is removed. Furthermore, the homogeneous representation of the IDE can be altered to a spatially heterogeneous representation allowing for the modelling and interpolation of more complex dynamics.

References

Aldroubi, A., Unser, M. & Aldroubi, A. (1994). Sampling procedures in function spaces and asymptotic equivalence with shannon's sampling

theory. *Numer. Funct. Anal. Optim. 15*(1-2), 1–21.

Chatfield, C. (2004). *The Analysis of Time Series: An Intoduction* (6th). CRC Press.

Eldar, Y. C. & Unser, M. (2006). Nonideal Sampling and Interpolation from Noisy Observations in Shift - Invariant Spaces. *IEEE Trans. Signal Process. 54*(7), 2636–2650.

Eldar, Y. C. & Werther, T. (2005). General Framework for Consistent Sampling in Hilbert Spaces. *Int. J. Wavelets, Multiresolution Inf. Process*, *3*(4), 497–509.

Feuer, A. (2004). On the Necessity of Papoulis' Result for Multidimensional GSE. *IEEE Trans. Signal Process. 11*(4), 420–422.

Izen, S. H. (2005). Generalised Sampling Expansion on Lattices. *IEEE Trans. Signal Process. 53*(6), 1949–1963.

Jr., J. L. B. & Sangsari, K. (1989). Sampling Reconstruction of N-Dimensional Band-Limited Images after Multilinear Filtering. *IEEE Trans. Circuits Syst. 36*(7), 1035–1038.

Kwok, C., Fox, D. & Meila, M. (2004). Real-Time Particle Filters. *Proc. IEEE*, *92*(3), 469–484.

McLachlan, G. J., Do, K.-A. & Ambroise, C. (2004). *Analyzing Microarray Gene Expression Data*. Wiley Series in Probability and Statistics. Hoboken, NJ, USA: John Wiley & Sons, Inc.

Medina, D., Moline, M., Clark, C. & Wood, J. Z. (2011). *Real - Time Visualizations of Ocean Data Collected by the NORUS Glider in Svalbard, Norway* (Master's thesis, California Polytechnic State University).

Nashed, M. Z. & Walter, G. G. (1991). General Sampling Theorems for Functions in Reproducing Kernel Hilbert Spaces. *Math. Control Signals Syst. 4*, 373–412.

Ozkan, E., Fritsche, C. & Gustafsson, F. (2012). Online EM Algorithm for Joint State and Mixture Measurement Noise Estimation. *Proc. IEEE Int. Conf. Inf. Fusion*, 1935–1940.

Papoulis, A. (1977). Generalized Sampling Expansion. *IEEE Trans. Circuit Syst. 24*, 652–654.

Petersen, D. P. & Middleton, D. (1962). Sampling and Reconstruction of Wave - Number - Limited Functions in N - Dimensonal Euclidean Spaces. *Inf. Control*, *5*, 279–323.

Petersen, D. P. & Middleton, D. (1964). Reconstruction of Multidimensional Stochastic Fields from Discrete Measurements of Amplitude and Gradient. *Inf. Control*, *7*, 445–476.

Poshtmasari, H. K., Sarvestani, Z. T., Kamkar, B., Shataei, S. & Sadeghi, S. (2012). Comparison of Interpolation Methods for Estimating pH and EC in Agricultural Fields of Golestan Province. *Int. J. Agric. Crop Sci. 4*(4), 157–167.

S. Ramani D. Van De Ville, T. B. & Unser, M. (2008). Nonideal Sampling and Regularization Theory. *IEEE Trans. Signal Process. 56*(3), 1055–1070.

Scerri, K., Dewar, M. & Kadirkamanathan, V. (2008). Estimation and Model Selection for an IDE-based Spatio-Temporal Model. *IEEE Trans. Signal Process. 57*(2), 482–492.

Schabenberger, O. & Gotway, C. A. (2005). *Statistical Methods for Spatial Data Analysis* (1st). CRC Press.

Shannon, C. E. (1949). Communication in the Presence of Noise. *37*, 10–21.

Unser, M. (2000). Sampling - 50 Years After Shannon. *IEEE Proc. 88*(4), 569–587.

Wan, E., van der Merwe & Nelson, A. (1999). Dual Estimation and the Unscented Transformation. In S. Solla, T. Leen & K.-R. Muller (Eds.), *Proc. neural inf. process. syst. conf.* (pp. 666–672). MIT Press.

Wikle, C. K. (2002). A kernel-based spectral model for non-Gaussian spatio-temporal processes. *Stat. Modelling*, *2*(4), 299–314.

Yao, K. (1967). Applications of Reproducing Kernel Hilbert Spaces - Band-Limited Models. *Inf. Control*, *11*, 429–444.